J Biomol NMR (2014) 58:165–173
DOI 10.1007/s10858-014-9814-6

ARTICLE

A fast NMR method for resonance assignments: application to metabolomics

Shivanand M. Pudakalakatti · Abhinav Dubey · Garima Jaipuria · U. Shubhashree · Satish Kumar Adiga · Detlef Moskau · Hanudatta S. Atreya

Received: 15 November 2013 / Accepted: 22 January 2014 / Published online: 2 February 2014

Abstract We present a new method for rapid NMR data acquisition and assignments applicable to unlabeled (^{12}C) or ^{13}C-labeled biomolecules/organic molecules in general and metabolomics in particular. The method involves the acquisition of three two dimensional (2D) NMR spectra simultaneously using a dual receiver system. The three spectra, namely: (1) G-matrix Fourier transform (GFT) (3,2)D [^{13}C, ^{1}H] HSQC–TOCSY, (2) 2D ^{1}H–^{1}H TOCSY and (3) 2D ^{13}C–^{1}H HETCOR are acquired in a single experiment and provide mutually complementary information to completely assign individual metabolites in a mixture. The GFT (3,2)D [^{13}C, ^{1}H] HSQC–TOCSY provides 3D correlations in a reduced dimensionality manner facilitating high resolution and unambiguous assignments. The experiments were applied for complete ^{1}H and ^{13}C assignments of a mixture of 21 unlabeled metabolites corresponding to a medium used in assisted reproductive technology. Taken together, the experiments provide time gain of order of magnitudes compared to the conventional data acquisition methods and can be combined with other fast NMR techniques such as non-uniform sampling and covariance spectroscopy. This provides new avenues for using multiple receivers and projection NMR techniques for high-throughput approaches in metabolomics.

Keywords GFT NMR · Multiple receivers · Metabolomics · 2D HSQC–TOCSY · Assisted reproductive technology

Electronic supplementary material The online version of this article (doi:10.1007/s10858-014-9814-6) contains supplementary material, which is available to authorized users.

S. M. Pudakalakatti · A. Dubey · G. Jaipuria · H. S. Atreya (✉)
NMR Research Centre, Indian Institute of Science, Bangalore 560012, India
e-mail: hsatreya@sif.iisc.ernet.in

S. M. Pudakalakatti · H. S. Atreya
Solid State and Structural Chemistry Unit, Bangalore 560012, India

A. Dubey
IISc Mathematics Initiative, Indian Institute of Science, Bangalore 560012, India

U. Shubhashree · S. K. Adiga
Clinical Embryology, Department of Obstetrics and Gynecology, Kasturba Medical College, Manipal University, Manipal 576104, India

D. Moskau
Bruker BioSpin AG, Industriestrasse 26, 8117 Faellanden, Switzerland

Introduction

One of the first steps in the analysis of an NMR spectrum of small molecules or a mixture of metabolites is the identification/resonance assignment of the individual components. This is accomplished typically using a set of homonuclear and heteronuclear two dimensional (2D) NMR spectra which includes 2D [^{13}C, ^{1}H] HSQC, 2D ^{1}H–^{1}H TOCSY and 2D [^{13}C, ^{1}H] HSQC–TOCSY (Cavanagh et al. 1996). In many cases to alleviate spectral overlap, a 3D ^{13}C-edited HSQC–TOCSY experiment helps in providing improved resolution by spreading the peaks in the third dimension. However, due to its high 'minimal' measurement time required for data acquisition the 3D NMR spectrum is seldom acquired for resonance assignment of small molecules/metabolites, especially for those which are not enriched with ^{13}C. To overcome this constraint several new approaches have been proposed in

recent years which provide considerable reductions in the measurement time required for acquiring high dimensional NMR spectra (Atreya and Szyperski 2005; Felli and Brutscher 2009; Schanda 2009; Coggins et al. 2010). While these methods have been successfully applied to biomolecules, their potential for small molecules or metabolites remains underutilized. Rapid data acquisition is particularly useful in metabolomics/systems biology, which often involves high-throughput profiling/analysis of metabolites in different bio-systems (Hawkins et al. 2010; Salgotra et al. 2013).

Two of the fast data acquisition methods include G-matrix Fourier transform (GFT) NMR spectroscopy (Kim and Szyperski 2003; Atreya and Szyperski 2004; Szyperski and Atreya 2006) and use of multiple NMR receivers for parallel data acquisition (Kupče et al. 2006, Kupče 2013). GFT NMR spectroscopy is a reduced dimensionality approach in which multiple chemical shifts are jointly sampled in the indirect dimension(s) of a *ND* experiment (Kim and Szyperski 2003; Atreya and Szyperski 2004; Szyperski and Atreya 2006). The reduction in dimensionality from *N*D to (*N*, *N*–*K*)D spectrum results when $K + 1$ chemical shifts are jointly sampled in one of the indirect dimensions. Time saving by an order of magnitude or more results from the fact that multiple chemical shifts are correlated in a single dimension instead of acquiring them in separate dimensions. A consequence of this is the detection of a linear combination of chemical shifts being sampled in the 'GFT dimension' instead of the individual chemical shifts themselves as in a conventional NMR spectrum (Atreya and Szyperski 2004; Szyperski and Atreya 2006). It is however straightforward to obtain the individual chemical shifts from the linear combination using either a simple addition/subtraction of the combinations or using a least square approach (Kim and Szyperski 2003). In addition to affording savings in measuring time, GFT NMR spectra have an additional advantage of having higher resolution than their parent *N*D spectrum. This is due to the fact that: (1) the reduction in the number of dimensions affords a longer acquisition time in the indirect dimension(s) (through collection of higher number of increments) resulting in narrower lines and (2) the sums and differences of chemical shifts resulting from joint sampling span a wider spectral range than the individual shifts themselves.

The second approach of parallel data acquisition using multiple NMR receivers is a more recent technical development in NMR spectroscopy (Kupče et al. 2006, 2007, 2010; Kupče and Freeman 2010a, b, 2011; Kupče and Wrackmeyer 2010; Kupče and Kay 2012; Donovan et al. 2013; Kupče 2013). The method involves the simultaneous or sequential acquisition of NMR time domain data [the free induction decay (FID)] of ^{1}H and heteronuclei (^{13}C/^{31}P/^{15}N/^{29}Si) by separate receiver systems. The individual FIDs are digitized, processed and stored separately allowing two NMR spectra to be acquired simultaneously. Different applications of this approach have been shown for small molecules (Kupče et al. 2006, 2007; Kupče and Freernan 2008, 2010a; Kupče 2013) and ^{13}C, ^{15}N labeled biomolecules (Kupče et al. 2010; Chakraborty et al. 2012; Kupče and Kay 2012; Reddy and Hosur 2013).

While the two approaches described above have been individually shown to provide time savings, their combination generates a powerful tool to accelerate data collection. Towards this end, we have developed a novel method wherein three 2D NMR spectra are acquired simultaneously in a single experimental data set using the dual receiver system for parallel data acquisition. Two of the spectra obtained using this method: (1) 2D ^{1}H–^{1}H TOCSY and (2) 2D ^{13}C–^{1}H HETCOR are based on the conventional data acquisition scheme and the third, namely, GFT (3,2)D ^{13}C-HSQC TOCSY is based on the GFT mode of data acquisition described above. To identify the experiments as acquired with a dual NMR receiver system, a prefix "DR" is added to the experimental name. In order to facilitate rapid assignment using the three spectra in concert, we have developed a (semi) automated approach. As discussed below, the three spectra provide mutually complementary information and aid in unambiguous resonance assignments. Compared to an equivalent high resolution set of conventional 3D HSQC–TOCSY, 2D ^{1}H–^{1}H TOCSY and 2D ^{13}C, ^{1}H spectra, the current method provides time savings of more than an order of magnitude. The data collection and analysis can be further accelerated by employing techniques such as non-uniform sampling (Hyberts et al. 2007, 2012) and covariance spectroscopy (Bruschweiler and Zhang 2004; Zhang and Brueschweiler 2004; Chen et al. 2006), which help to provide high resolution in the indirect dimensions. The method is applied to a mixture of 21 metabolites comprising a medium used in human in vitro fertilization (IVF) and is applicable to molecules/metabolites either in unlabeled (natural ^{13}C abundance) or ^{13}C enriched forms. In particular, the method will be of high utility in metabolomics for rapid analysis (Lindon et al. 2000; Nagana Gowda et al. 2012).

Methods and materials

Implementation of NMR experiments

Figure 1 depicts the flow of magnetization in the experiment proposed and the chemical shift correlations observed. Briefly, all ^{1}H spins (attached to ^{12}C or ^{13}C) are frequency labeled during 't_1' in the first INEPT step in a semi-constant time manner. Simultaneously during this

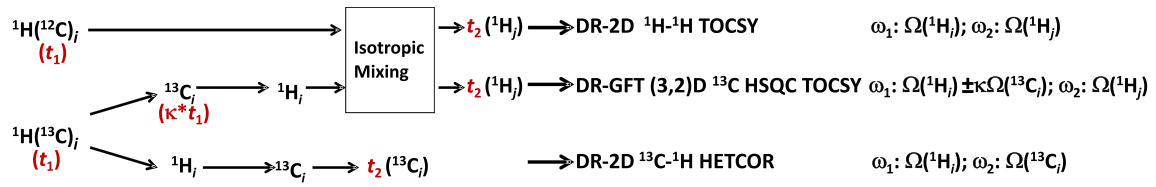

Fig. 1 A schematic depiction of the magnetization pathway implemented in the proposed experiments. The chemical shift correlations observed in each of the experiments are indicated

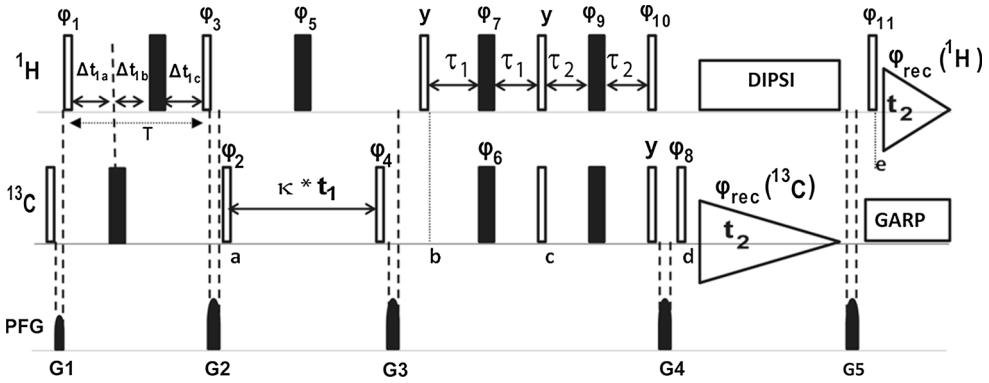

Fig. 2 R.f. pulse scheme for acquiring dual receiver (DR) GFT (3,2)D ^{13}C HSQC–TOCSY, DR-2D ^1H–^1H TOCSY and DR-2D [^{13}C, ^1H] HETCOR in a single experimental data set. The magnetization transfer scheme is illustrated in Fig. 1. *Thin* and *thick vertical bars* indicate rectangular 90° and 180° pulses, respectively, and the RF phases are indicated above the pulses. Where no r.f. phase is marked, the pulse is applied along *x*. High power 90° pulse lengths are 9 μs for ^1H and 12 μs for ^{13}C in the solution state. The ^{13}C r.f. carrier is placed at 40 ppm and the ^1H carrier position is set to 4.7 ppm throughout the duration of the experiment. Chemical shift evolution of ^1H during t_1 is carried out in a semi-constant time manner. The initial values ($t_1 = 0$) of t_{1a} (0), t_{1b} (0) and t_{1c} (0) are: 0.9 ms, 3 μs and 0.9 ms, respectively ($1/(8^1J_{HC})$; $^1J_{HC} \sim 140$ Hz) such that T = 1.8 ms. For semi-constant time evolution, the values of Δt_{1b} and Δt_{1c} are based on the number of increments and the spectral width. For 512 complex points and spectral width of 20,000 Hz (25 ppm) used for the indirect (^1H) dimension in the current study, the values of Δt_{1a}, Δt_{1b} and Δt_{1c} are: 25, 23.3 and −1.7 μs. The chemical shift evolution period of ^{13}C during t_1 is co-incremented with that of ^1H with a relative scaling factor (κ). GARP is employed to decouple ^{13}C from ^1H. A ^{13}C spectral width of 200 ppm is chosen for the direct dimension (in 2D HETCOR) and 25 ppm for the indirect dimension (in GFT (3,2)D HSQC TOCSY and 2D ^1H–^1H TOCSY). A mixing time of 80 ms is use for isotropic mixing of ^1H with DIPSI. The delays are : $\tau_1 = 1.8$ ms, $\tau_2 = 0.9$ ms. Phase cycling: $\phi_1 = x$; $\phi_2 = x$; $\phi_3 = y$, $-y$; $\phi_4 = x, -x$; $\phi_5 = x, x, -x, -x$; $\phi_6 = x, x, -x, -x$; $\phi_7 = x, -x$; $\phi_8 = x, x, -x, -x$; $\phi_9 = x, x, -x, -x$; $\phi_{10} = x, -x$; $\phi_{11} = x, x, -x, -x$; ϕ(rec) (^{13}C) = *x, x, −x, −x*; ϕ(rec) (^1H) = *x, −x, −x, x*. The PFGs applied have Sinc shaped with strengths: G1 = 19 G/cm; G2 = 19 G/cm; G3 = 19 G/cm; G4 = 19 G/cm; G5 = 11 G/cm; Quadrature detection in t_1 (^1H) out in States manner (i.e., $\phi_1 = x, y$). See text for data processing and analysis

period, the magnetization of ^1H attached to ^{13}C branches out into two parts: one part being transferred to ^{13}C and the remaining retained on ^1H (this can be achieved by tuning the INEPT delay to $1/4J_{HC}$ instead of $1/2J_{HC}$). The part of the ^1H magnetization that is retained is utilized later down the sequence to transfer to ^{13}C for acquiring 2D HETCOR. The part which is transferred to ^{13}C is frequency labeled again (in t_1) for joint sampling with ^1H with a relative scaling factor (κ). The magnetization of ^1H attached to ^{12}C is retained throughout the pulse sequence and subjected (along with ^1H attached to ^{13}C) to isotropic mixing for observing the TOCSY correlations during t_2. Thus, three spectra are acquired (in an interleaved manner), which provide the different chemical shifts correlations as depicted in Fig. 1. The DR-2D ^1H–^1H TOCSY is indeed obtained for "free" within the scans used for signal averaging and artifact suppression and together with DR-2D HETCOR serves as the 'central peak spectrum' for the GFT spectrum (Kim and Szyperski 2003). The radio frequency (r.f.) pulse scheme for the experiments are shown in Fig. 2 and the various product operators terms observed at different points along the r.f. pulse sequence is given in Table 1 for unlabeled (^{12}C) molecules. A plot of transfer function as a function of the delay periods (T, τ_1, τ_2 in Fig. 1) is shown in Figure S2.

In a ^{13}C-labeled sample the 2D ^1H–^1H TOCSY is obtained either from any ^1H bound to ^{12}C or from ^1H magnetization arising from incomplete transfer of magnetization of ^1H to ^{13}C during the ^1H-^{13}C polarization transfer steps in the r.f. pulse sequence. Thus, the sensitivity of 2D ^1H–^1H TOCSY in ^{13}C labeled samples can be adjusted to the desired levels by modifying the delay periods (T, τ_1, τ_2 in Fig. 2) used for ^1H–^{13}C magnetization transfer. The flow of magnetization for a ^{13}C-labeled sample is depicted in

Table 1 Coherences and Transfer amplitudes along the r.f. pulse sequence (Fig. 2)

Points along r.f. pulse sequence	GFT (3,2)D ^{13}C-HSQC TOCSY[a]	2D ^{1}H–^{1}H TOCSY[b]	2D ^{13}C–^{1}H HETCOR
a	$-2I_ZS_Y$ *$\sin(\pi^1J_{HC}T)$ *$\exp(i\Omega_{Hi}t_1)$	I_Y *$\exp(i\Omega_{Hi}t_1)$	I_Y *$\cos(\pi^1J_{HC}T)$ *$\exp(i\Omega_{Hi}t_1)$
b	$-2I_XS_Z$ *$\sin(\pi^1J_{HC}T)$ *$\exp(i\Omega_{Hi}t_1)$ *$\exp(i\kappa\Omega_{Ci}t_1)$	$-I_Y$ *$\exp(i\Omega_{Hi}t_1)$	$-I_Y$ *$\cos(\pi^1J_{HC}T)$ *$\exp(i\Omega_{Hi}t_1)$
c	I_Y *$\sin(\pi^1J_{HC}T)$ *$\exp(i\Omega_{Hi}t_1)$ *$\exp(i\kappa\Omega_{Ci}t_1)$ *$\sin(\pi^1J_{HC}*2\tau_1)$	I_Y *$\exp(i\Omega_{Hi}t_1)$	$-2I_ZS_Y$ *$\cos(\pi^1J_{HC}T)$ *$\exp(i\Omega_{Hi}t_1)$ *$\sin(\pi^1J_{HC}*2\tau_1)$
d	I_Z *$\sin(\pi^1J_{HC}T)$ *$\exp(i\Omega_{Hi}t_1)$ *$\exp(i\kappa\Omega_{Ci}t_1)$ *$\sin(\pi^1J_{HC}*2\tau_1)$ *$\cos(\pi^1J_{HC}*2\tau_2)$	$-I_Z$ *$\exp(i\Omega_{Hi}t_1)$	S_Y *$\cos(\pi^1J_{HC}T)$ *$\exp(i\Omega_{Hi}t_1)$ *$\sin(\pi^1J_{HC}*2\tau_1)$ *$\sin(\pi^1J_{HC}*2\tau_2)$ *Σ_i $\cos(\pi^1J_{HiC}*2\tau_2)$
e	$-\Sigma_j\ I_{Yj}$ * [$\sin(\pi^1J_{HC}T)$ *$\exp(i\Omega_{Hi}t_1)$ *$\exp(i\kappa\Omega_{Ci}t_1)$ *$\sin(\pi^1J_{HC}*2\tau_1)$ *$\cos(\pi^1J_{HC}*2\tau_2)$]	$\Sigma_j\ I_{Yj}$ * *$\exp(i\Omega_{Hi}t_1)$	
Detection (t_2)	$\Sigma_j \exp(i\Omega_{Hj}t_2)$* [$\sin(\pi^1J_{HC}T)$ *$\exp(i\Omega_{Hi}t_1)$ *$\exp(i\kappa\Omega_{Ci}t_1)$ *$\sin(\pi^1J_{HC}*2\tau_1)$ *$\cos(\pi^1J_{HC}*2\tau_2)$]	$\exp(i\Omega_{Hi}t_1)$* Σ_j $\exp(i\Omega_{Hj}t_2)$	$\exp(i\Omega_{Ci}t_2)$ *$\cos(\pi^1J_{HC}T)$ *$\exp(i\Omega_{Hi}t_1)$ *$\sin(\pi^1J_{HC}*2\tau_1)$ *$\sin(\pi^1J_{HC}*2\tau_2)$

[a] T is the total ^{1}H–^{13}C transfer delay period (=1/4J_{HC}) during the semi-constant evolution in t_1 (Fig. 2)

[b] For ^{1}H bound to ^{12}C (Fig. 1). For ^{13}C labeled samples, the transfer function is given in Table S2

Figure S1 and the various product operators terms observed at different points along the r.f. pulse sequence is given in Table S2.

For acquiring GFT data, the chemical shift evolution period of ^{13}C is co-incremented with that of ^{1}H and detected in quadrature using the States method by varying $\phi_2 = x, y$ (Fig. 2). The four FIDs thus collected by varying ϕ_1 and ϕ_2 independently, are collected separately and pre-processed using the G-matrix prior to Fourier transform (Atreya and Szyperski 2005). This results in the linear combination of chemical shifts of $^{1}H_i$ and its directly attached $^{13}C_i$ nucleus along ω_1, whereas in the direct dimension (ω_2) $^{1}H_j$ shift correlations as in a conventional 2D ^{1}H–^{1}H TOCSY are detected (Fig. 1). The GFT experiment thus provides chemical shift correlations observed in a 3D ^{13}C-edited HSQC–TOCSY. The FIDs corresponding to the two spectra: GFT (3,2)D HSQC–TOCSY and 2D TOCSY are acquired simultaneously. Their separation into different spectra is accomplished by recording two sets of interleaved data with $\phi_4 = x$, and $-x$ (Fig. 2). In the two data sets acquired, the FIDs of GFT (3,2)D HSQC TOCSY and 2D TOCSY have the same and opposite phase, respectively. The two sets of FIDs are then added/subtracted to yield separate FIDs for GFT (3,2)D HSQC TOCSY and 2D TOCSY. The 2D ^{13}C-^{1}H HETCOR is acquired in parallel as a separate data set and directly Fourier transformed. This spectrum provides chemical shift correlations equivalent to a ^{1}H detected 2D [^{13}C, ^{1}H] HSQC.

Analysis of NMR experiments

The peak pattern/shift correlations observed in the three different spectra (Fig. 1) facilitates an easy/automated approach to resonance assignments. The three spectra are analyzed in concert as follows. Starting from a given cross peak (C_i,H_i) in DR-2D [^{13}C, ^{1}H] HETCOR, peaks ($^{1}H_j$) in the two DR-GFT (3,2)D ^{13}C-HSQC TOCSY sub-spectra are identified that have $\Omega(^{1}H_i) \pm \kappa*\Omega(^{13}C_i)$ chemical shifts in the GFT (ω_1) dimension and $\Omega(^{1}H_j)$ in the ω_2 dimension within a given tolerance. The cross peaks ($^{1}H_j$) thus identified are validated using DR-2D TOCSY in which they are expected to be observed along the ω_2 dimension corresponding to $\Omega(^{1}H_i)$ in the ω_1 dimension. After identifying the correct ($^{1}H_j$) resonances, the respective (C_j,H_j) peaks in the DR-2D [^{13}C, ^{1}H] HETCOR are identified and the process repeated with search of new cross peaks in the two GFT DR-(3,2)D ^{13}C-HSQC TOCSY spectra that have $\Omega(^{1}H_j) \pm \kappa*\Omega(^{13}C_j)$ chemical shifts in the GFT (ω_1) dimension. A potential ambiguity can arise while identifying the cross peak corresponding to (C_j,H_j) from DR-2D [^{13}C, ^{1}H] HETCOR based only on $\Omega(^{1}H_j)$. For instance, several H_j may have similar C_j shift values. In such a case, the two DR-GFT (3,2)D ^{13}C-HSQC TOCSY sub-spectra are analyzed for the presence of a cross peak at $\Omega(^{1}H_i)$ in the ω_2 dimension and $\Omega(^{1}H_j) \pm \kappa*\Omega(^{13}C_j)$ chemical shifts in the ω_1 dimension. This corresponds to the transpose/reciprocal peak for the cross peak at ω_1: $\Omega(^{1}H_i) \pm \kappa*\Omega(^{13}C_i)$ and ω_2: $\Omega(^{1}H_j)$ identified in the previous step. This ambiguity can also be resolved using the covariance spectroscopy described below (see Results and Discussion). Once the correct (C_j,H_j) is identified the process is iterated until all CH moieties in one spin-system are identified and assigned. The assignment of the spin system to the corresponding

metabolite can be done using the chemical shift database available in BioMagResBank. The entire process can be automated using just the peak lists obtained from the three 2D spectra. The relevant scripts can be downloaded from http://nrc.iisc.ernet.in/hsa/softwares.

Sample preparation and NMR data collection

All NMR experiments were performed at 20 °C on a Bruker Avance III (HD) spectrometer operating at a ^{1}H resonance frequency of 800 MHz and equipped with a cryogenic probe and a dual receiver system. The experiments were carried out at natural ^{13}C abundance with a sample prepared in $^{2}H_2O$ comprising a mixture of the following 21 metabolites each of 5–7 mM concentration: Alanine, Arginine, Asparagine, Cysteine, Glucose, Glutamine, Histidine, Lactate, Lysine, Isoleucine, Leucine, Methionine, Phenylalanine, Proline, Pyruvate, Serine, Taurine, Threonine, Tryptophan, Tyrosine, and Valine. This sample was prepared to assign the metabolites of the original innovative sequential medium-1 (ISM1) medium, which has been used previously for profiling and culturing the human embroys for IVF (Pudakalakatti et al. 2013; Xella et al. 2010) but the individual components of which were not assigned completely.

The data (comprising the three 2D spectra together) was acquired with a spectral width of 25 ppm in the indirect (GFT/TOCSY) dimension in a total measurement time of 10.5 h with an acquisition time (t_{max}) of ~13 ms in the indirect dimension and scaling factor: $\kappa = 1$ (complete details of acquisition parameters are given in Table S1). The raw data (FID) was pre-processed as described above. After pre-processing, the FID was apodized using cosine function and zero filled to 2,048 points prior to Fourier transform.

Results and discussion

Assignments of metabolites in ISM1 medium

Figure 3 shows the three 2D spectra obtained for the ISM1 mixture at natural ^{13}C abundance. Nearly 92 % of the expected number of peaks (61) were observed in DR-2D [^{13}C, ^{1}H] HETCOR. The peak yield for the DR-2D TOCSY and DR-GFT (3,2)D ^{13}C HSQC–TOCSY spectrum was ~92 %. An example illustrating the resonance assignment of lysine across the three spectra is shown in Fig. 3. Complete chemical shift assignments of the metabolites obtained by analyzing the three spectra are given in Table S3 of Supporting Information. The assignments marked on the 2D [^{13}C, ^{1}H] HSQC spectra of the ISM1 medium is shown in Figure S3 of Supporting Information.

The GFT spectra alleviates spectral overlap as illustrated in Fig. 4. In the 2D ^{13}C HSQC–TOCSY spectrum, for any two or more CH pairs (from different molecules) which have distinct ^{1}H chemical shifts but degenerate ^{13}C shifts, the TOCSY correlations overlap in the direct dimension (ω_2) as illustrated in Fig. 4a. This degeneracy in ^{13}C shifts is removed in the GFT spectra (Fig. 4a; right) when the ^{1}H shifts are added/subtracted to their directly attached ^{13}C shifts. Thus, the ^{1}H shifts correlating to the individual CH spin systems in the direct dimension (ω_2) can be unambiguously identified. This is further illustrated in Fig. 4b using the DR-GFT (3,2)D ^{13}C HSQC–TOCSY spectrum of the 21 metabolite mixture. Two of the metabolites (methionine and lysine) in the mixture have similar $^{13}C^{\beta}$ shifts. They are therefore overlapped in the ω_1 dimension of a conventional 2D ^{13}C HSQC TOCSY (left). However, due to the differences in their $^{1}H^{\beta}$ shifts, they are resolved in the DR-GFT (3,2)D ^{13}C HSQC–TOCSY (right) facilitating unambiguous assignments.

An analysis of the 902 ^{1}H and ^{13}C chemical shifts from 315 metabolites observed in the blood sample (obtained from BioMagResBank; http://www.bmrb.wisc.edu) reveals that ~96 % of all ^{13}C shifts of CH pairs from one molecule overlap within ±0.2 ppm (but ^{1}H shifts separated by ±0.02 ppm) with ^{13}C shifts of at least another CH pair from same or different molecule. However, when the chemical shifts of ^{1}H and ^{13}C are combined in the GFT experiment as shown in Fig. 3, this overlap is reduced to ~30 %.

Sensitivity and resolution considerations

The signal-to-noise distribution of cross peaks observed in the three spectra (shown in Fig. 3) are given in Figure S4 of Supporting Information. In the case of unlabeled (non-^{13}C enriched) molecules, among the three spectra 2D TOCSY has the highest sensitivity due to high abundance of ^{1}H attached to ^{12}C (99 %); whereas in ^{13}C-enriched molecules, the 2D TOCSY has the least sensitivity compared to the other two spectra due to lower abundance of ^{1}H bound to ^{12}C (Figure S5). In such samples, the 2D ^{1}H-^{1}H TOCSY is obtained either from any ^{1}H bound to ^{12}C or from residual ^{1}H magnetization arising from its incomplete transfer to ^{13}C during the ^{1}H–^{13}C polarization transfer steps with delay periods, T, τ_1 and τ_2, in the r.f. pulse sequence (Fig. 2; Table S2). This was verified experimentally by acquiring two spectra with ^{13}C-labeled proline: one with the delay period $\tau_1 = 1.8$ ms (corresponding to $1/4^{1}J_{HC}$; $J_{HC} = 140$ Hz) and other with $\tau_1 = 0.8$ ms (corresponding to $\sim 1/10^{1}J_{HC}$). The S/N of the 2D TOCSY was significantly enhanced, whereas a ~30 % drop in sensitivity of the GFT and 2D HETCOR spectra was observed as expected from their transfer functions (Figure S2). Thus,

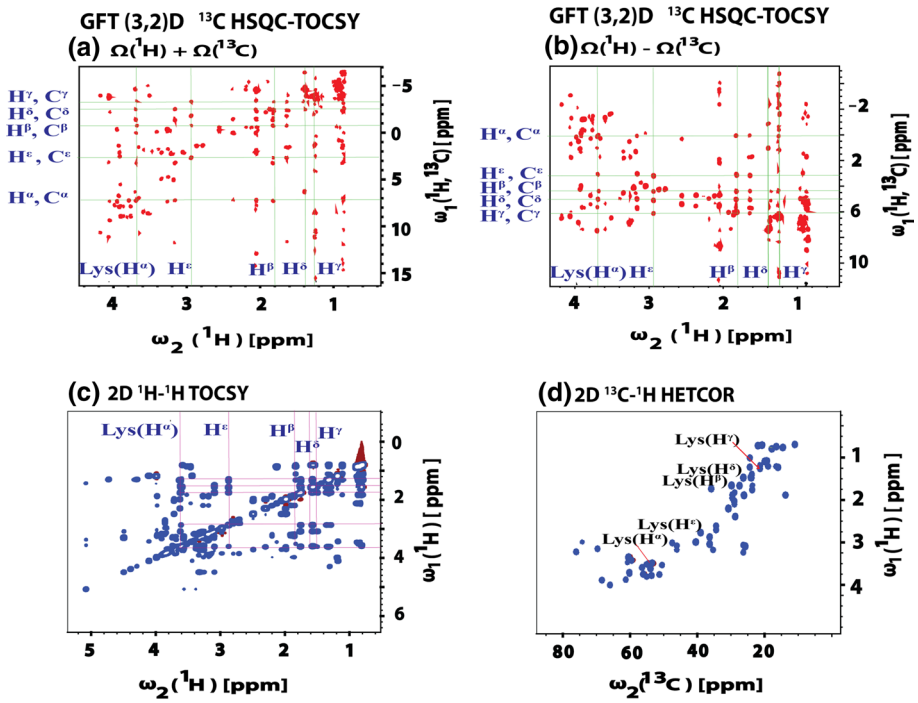

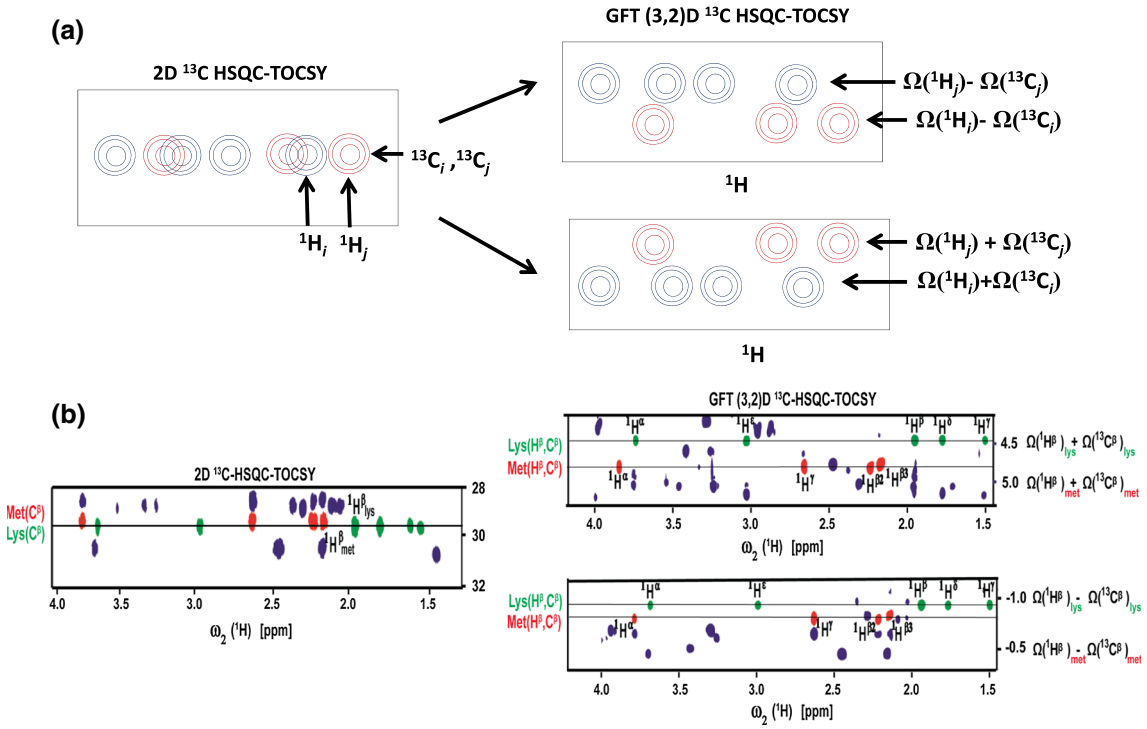

Fig. 3 **a**, **b** DR-GFT (3,2)D ^{13}C HSQC–TOCSY, **c** DR-2D ^{1}H–^{1}H TOCSY and **d** DR-2D HETCOR spectra acquired for the mixture of 21 metabolites comprising the ISM1 medium in 10.5 h at natural ^{13}C abundance (each metabolite has a concentration of ~5 to 7 mM). For the purpose of illustration of the peak pattern observed, the spin-system corresponding to lysine is shown in the three spectra. The complete assignment of the metabolites obtained using this set of spectra is given in Table S3 of Supporting Information. The assignment mapped on the 2D ^{13}C–^{1}H HSQC spectrum of the ISM1 medium in shown in Figure S3 of Supporting Information

Fig. 4 **a** An illustration of spectral overlap in a conventional 2D HSQC–TOCSY which is resolved in GFT (3,2)D HSQC–TOCSY. If two CH pairs, '*i*' and '*j*' have similar $^{13}C_i$ and $^{13}C_j$ chemical shifts but different $^{1}H_i$ and $^{1}H_j$ shifts, the ^{1}H correlations of spin system corresponding to *i* and *j* overlap in the ω_1 (^{13}C) dimension (as shown on the *left*). They are separated in the GFT (3,2)D HSQC–TOCSY (shown on *right*) due to the detection of linear combinations: $\Omega(^{1}H) \pm \Omega(^{13}C)$ which is different for *i* and *j*. **b** An illustration of spectral overlap of two spin systems (methione and lysine) in the conventional 2D HSQC–TOCSY for the mixture of 21 metabolites used in the study which is resolved in GFT (3,2)D HSQC–TOCSY (as illustrated in Fig. 3). On *left* is shown the overlap of spin systems of methionine and lysine that have similar $^{13}C^{\beta}$ chemical shift but different $^{1}H^{\beta}$ shifts. They are separated in the GFT (3,2)D HSQC–TOCSY due to the detection of linear combinations: $\Omega(^{1}H) \pm \Omega(^{13}C)$ shifts (shown on the *right* with peaks belonging to methionine colored in *red* and lysine in *green* for clarity)

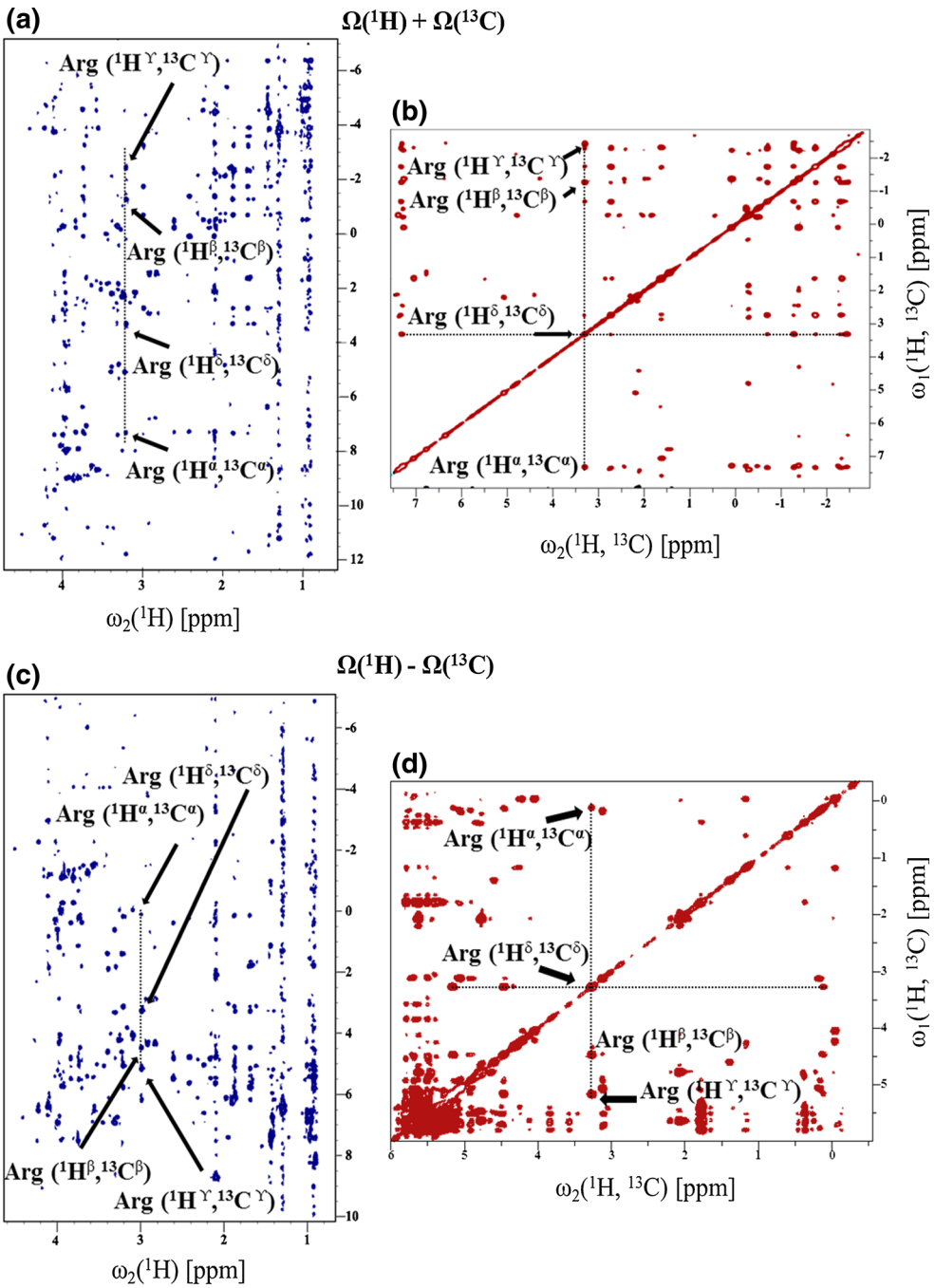

Fig. 5 Transformation of DR-GFT (3,2)D HSQC–TOCSY to a new 2D spectrum using indirect covariance spectroscopy resulting in GFT shift combinations observed in both the dimensions. The DR-GFT (3,2)D HSQC–TOCSY spectrum acquired for the 21 metabolite mixture (Fig. 3) is shown in **a**, **c** corresponding to the two linear combinations: $\Omega(^1H) + \Omega(^{13}C)$ and $\Omega(^1H) - \Omega(^{13}C)$. The respective new DR-GFT (3,2)D covariance HSQC–TOCSY spectra obtained using the MATLAB scripts described in Short et al. 2011 is shown in **b**, **d**. The ^1H, ^{13}C correlations of arginine at $^1H^{\delta}$, $^{13}C^{\delta}$ are highlighted as an illustration

the sensitivity of 2D ^1H–^1H TOCSY in ^{13}C labeled samples can be adjusted to the desired levels by modifying the delay periods used for ^1H–^{13}C polarization transfers. Further, in samples enriched with ^{13}C, a constant time version of the experiment can be used to avoid loss in resolution due to one bond ^{13}C–^{13}C scalar couplings. In comparison to a non-dual receiver GFT (3,2)D ^{13}C HSQC–TOCSY, the sensitivity loss of a factor of $\sqrt{2}$ in DR-GFT (3,2)D ^{13}C HSQC–TOCSY occurs primarily due to the branching of the magnetization ^1H attached to ^{13}C into two pathways (Figs. 1, 2; ^1H–^{13}C transfer delay period for the first INEPT step is set to 1/4 J compared to 1/2 J as in a conventional ^{13}C HSQC–TOCSY). Further, the GFT (3,2)D spectrum has a factor 2 less in sensitivity compared to a conventional 2D ^{13}C- HSQC TOCSY due to splitting of peaks into the two linear combinations and factor of $\sqrt{2}$ compared to a 3D ^{13}C-edited HSQC TOCSY. For samples limited in sensitivity, this method can be combined with other approaches which provide enhanced sensitivity in metabolomics (Nagana Gowda et al. 2012).

The GFT spectra, however, have high resolution compared to the parent 3D ^{13}C-edited HSQC–TOCSY due to two factors. First, the cross peaks in the indirect dimension have narrower linewidths due to longer chemical shift acquisition periods (t_{max}) in the GFT dimension (ω_1) compared to that feasible practically in the 3D experiment. For acquiring data at natural ^{13}C abundance t_{max} is limited only by T_2 relaxation (we have used a t_{max} of $\sim$13 ms). However, there is an option of scaling the chemical shifts of ^{13}C relative to that of ^{1}H (Fig. 1). This is useful in the case of ^{13}C enriched molecules, wherein a lower t_{max} (<8 ms) for ^{13}C shift evolution needs to be considered to avoid the effects of one bond ^{13}C–^{13}C scalar couplings ($\sim$35 Hz) if a non-constant mode of shift evolution is chosen. Second, peaks in the GFT experiments are spread over a higher spectral range compared to the parent 3D experiment. The spectral width in the ω_1 (GFT) dimension is the sum of the spectral widths of ^{1}H and ^{13}C with appropriate scaling (i.e., SW_{tot} $(\omega_1) = SW(^{1}H) + \kappa*SW(^{13}C)$) (Szyperski and Atreya 2006). For a scaling factor of 1.0, typically a spectral width of 25–30 ppm in ^{1}H (equivalent to 100–120 ppm for ^{13}C) results considering both the linear combinations ($\Omega(^{1}H) \pm \kappa*\Omega(^{13}C)$) compared to a typical range of 80–100 ppm for ^{13}C shifts required for a conventional 2D ^{13}C-edited HSQC–TOCSY.

Analysis of spectra using covariance spectroscopy

The three spectra provide mutually complementary shift correlations, which facilitates automated analysis of the spectra as discussed above. The analysis of the DR-(3,2)D GFT spectra can be further boosted using the indirect covariance spectroscopy (Zhang and Brueschweiler 2004). In this approach, the chemical shift correlations observed 'along' the indirect dimension of a 2D spectrum is transformed to the direct dimension. While the information content is similar to that of the originally acquired data, the new spectrum provides an easy approach to 'track' the chemical shift correlations (Zhang and Brueschweiler 2004).

This approach was tested for DR-GFT (3,2)D spectra of the mixture of 21 metabolites used in the study. The transformed GFT sub-spectra [named as DR-GFT (3,2)D Covariance HSQC–TOCSY) are shown in Fig. 5b, d, where both the dimensions now encode the linear combination of ^{1}H and ^{13}C shifts ($\Omega(^{1}H) \pm \Omega(^{13}C)$] observed originally in the indirect dimension of the DR-GFT (3,2)D spectra (Fig. 5a, c). The analysis of the spectrum is simplified by the fact that starting with a given (C_i,H_i) chemical shift from 2D HETCOR, the (C_j,H_j) shifts corresponding to the proton, $^{1}H_j$, which is connected to $^{1}H_i$ by TOCSY can be traced out along the direct or the indirect dimension of the newly transformed DR-GFT (3,2)D Covariance HSQC–TOCSY. This is illustrated for the spin system of arginine in Fig. 5b, d. The GFT spectrum is thus transformed into a one providing 4D shift correlations (i.e., H_i, C_i, H_j, C_j), which is otherwise practically impossible to acquire rapidly at natural ^{13}C abundance. This facilitates an easy way to analyze (especially for automation) the GFT spectrum.

Conclusions

We have developed a new experiment which provides three NMR spectrum in a single experimental data set for resonance assignments of molecules. The methodology combines two rapid data acquisition methods, namely, GFT NMR spectroscopy and the multiple NMR receiver system. In comparison to an equivalent high resolution set of conventionally acquired 3D HSQC–TOCSY, 2D ^{1}H–^{1}H TOCSY and 2D ^{13}C, ^{1}H spectra, the current method provides time savings of an order of magnitude. The method is applicable to any bio/organic molecule (peptides or metabolites) or a mixture of small molecules either in unlabeled (^{12}C) or ^{13}C labeled form. The analysis of the GFT spectrum is facilitated using indirect covariance spectrum, which transforms the spectrum to one providing direct (C_i,H_i) to (C_j,H_j) shift correlations within a molecule. This is the first application of GFT NMR spectroscopy for resonance assignment of small molecules and will be particularly useful in metabolomics for high throughput analysis.

Acknowledgments The facilities provided by NMR Research Centre at IISc supported by Department of Science and Technology (DST), India is gratefully acknowledged. HSA acknowledges research support from Department of Atomic Energy, India. SA acknowledges research support from DST. AD acknowledges fellowship from Council of Scientific and Industrial Research (CSIR).

References

Atreya HS, Szyperski T (2004) G-matrix Fourier transform NMR spectroscopy for complete protein resonance assignment. Proc Natl Acad Sci USA 101:9642–9647

Atreya HS, Szyperski T (2005) Rapid NMR data collection. Methods Enzymol 394:78–108

Bruschweiler R, Zhang FL (2004) Covariance nuclear magnetic resonance spectroscopy. J Chem Phys 120:5253–5260

Cavanagh J, Fairbrother WJ, Palmer AG, Skelton NJ (1996) Protein NMR spectroscopy. Academic Press, San Diego, CA

Chakraborty S, Paul S, Hosur RV (2012) Simultaneous acquisition of $^{13}C\alpha$–^{15}N and ^{1}H–^{15}N–^{15}N sequential correlations in proteins: application of dual receivers in 3D HNN. J Biomol NMR 52:5–10

Chen YB, Zhang FL, Bermel W, Bruschweiler R (2006) Enhanced covariance spectroscopy from minimal datasets. J Am Chem Soc 128:15564–15565

Coggins BE, Venters RA, Zhou P (2010) Radial sampling for fast NMR: concepts and practices over three decades. Prog NMR Spectrosc 57:381–419

Donovan KJ, Kupče E, Frydman L (2013) Multiple parallel 2D NMR acquisitions in a single scan. Angew Chem Int Ed 52:4152–4155

Felli IC, Brutscher B (2009) Recent advances in solution NMR: fast methods and heteronuclear Direct Detection. ChemPhysChem 10:1356–1368

Hawkins RD, Hon GC, Ren B (2010) Next-generation genomics: an integrative approach. Nat Rev Genet 11:476–486

Hyberts SG et al (2007) Ultrahigh-resolution ^{1}H–^{13}C HSQC spectra of metabolite mixtures using nonlinear sampling and forward maximum entropy reconstruction. J Am Chem Soc 129:5108–5116

Hyberts SG, Arthanari H, Wagner G (2012) Applications of non-uniform sampling and processing. Top Curr Chem 316:125–148

Kim S, Szyperski T (2003) GFT NMR, a new approach to rapidly obtain precise high-dimensional NMR spectral information. J Am Chem Soc 125:1385–1393

Kupče E (2013) NMR with multiple receivers. Top Curr Chem 335:71–96

Kupče E, Freeman R (2010a) Molecular structure from a single NMR sequence (fast-PANACEA). J Magn Reson 206:147–153

Kupče E, Freeman R (2010b) High-resolution NMR correlation experiments in a single measurement (HR-PANACEA). Magn Reson Chem 48:333–336

Kupče E, Freeman R (2011) Parallel receivers and sparse sampling in multidimensional NMR. J Magn Reson 213:1–13

Kupče E, Freernan R (2008) Molecular structure from a single NMR experiment. J Am Chem Soc 130:10788–10792

Kupče E, Kay LE (2012) Parallel acquisition of multi-dimensional spectra in protein NMR. J Biomol NMR 54:1–7

Kupče E, Wrackmeyer B (2010) Multiple receiver experiments for NMR spectroscopy of organosilicon compounds. App Org Chem 24:837–841

Kupče E, Freeman R, John BK (2006) Parallal acquisition of two-dimensional NMR spectra of several nuclear species. J Am Chem Soc 128:9606–9607

Kupče E, Cheatham S, Freeman R (2007) Two-dimensional spectroscopy with parallel acquisition of H-1-X and F-19-X correlations. Magn Reson Chem 45:378–380

Kupče E, Kay LE, Freeman R (2010) Detecting the "afterglow" of 13C NMR in proteins using multiple receivers. J Am Chem Soc 132:18008–18011

Lindon JC, Nicholson JK, Holmes E, Everett JR (2000) Metabolomics process studied by NMR spectroscopy of biofluids. Concepts Magn Reson 12:289–320

Nagana Gowda GA, Shanaiah N, Raftery D (2012) Isotope enhanced approaches in metabolomics. In: Atreya HS (ed) Isotope labeling in biomolecular NMR. Springer, Netherlands, pp 147–164

Pudakalakatti SM, Uppangala S, D'Souza F, Kalthur G, Kumar P, Adiga SK, Atreya HS (2013) NMR studies of preimplantation embryo metabolism in human assisted reproductive techniques: a new biomarker for assessment of embryo implantation potential. NMR Biomed 26:20–27

Reddy JG, Hosur RV (2013) Parallel acquisition of 3D-HA(CA)NH and 3D-HACACO spectra. J Biomol NMR 56:77–84

Salgotra RK, Gupta BB, Stewart CN, Jr (2013) From genomics to functional markers in the era of next-generation sequencing. Biotechnol Lett

Schanda P (2009) Fast-pulsing longitudinal relaxation optimized techniques: enriching the toolbox of fast biomolecular NMR spectroscopy. Prog NMR Spectrosc 55:238–265

Short T, Alzapiedi L, Bruschweiler R, Snyder D (2011) A covariance NMR toolbox for MATLAB and OCTAVE. J Magn Reson 209:75–78

Szyperski T, Atreya HS (2006) Principles and applications of GFT projection NMR spectroscopy. Magn Reson Chem 44:S51–S60

Xella S, Marsella T, Tagliasacchi D, Giulini S, La Marca A, Tirelli A, Volpe A (2010) Embryo quality and implantation rate in two different culture media: ISM1 versus Universal IVF medium. Fertil Steril 93:1859–1863

Zhang F, Brueschweiler R (2004) Indirect covariance NMR spectroscopy. J Am Chem Soc 126:13180–13181